SKS/SKKS splitting and Taiwan orogeny

Hao Kuo-Chen,[1] Francis T. Wu,[1] David Okaya,[2] Bor-Shouh Huang,[3] and Wen-Tzong Liang[3]

Received 17 March 2009; revised 8 May 2009; accepted 12 May 2009; published 16 June 2009.

[1] We determine 58 sets of splitting parameters, fast direction (φ) and delay time (δt), from broadband SKS/SKKS waves recorded at temporary and permanent stations in Taiwan. These and earlier results, from S and ScS as well as SKS, show an island-wide pattern of φ alignment with N–NNE structural trends in southern and central Taiwan and then turn smoothly to EW following the structural bight in northern Taiwan. Remarkable differences in δt for eastern and southwestern events are found, resulting probably from a more anisotropic upper mantle in the east, under the Central Range. With δt an average of 1.3 seconds our observations are consistent with the hypothesis that the orogeny involves shear or flow in the upper mantle in central and southern Taiwan. In northern Taiwan, near the ends of the collision and subduction zones, the extrusion and the hydration of olivine may contribute to the orientation of φ. **Citation:** Kuo-Chen, H., F. T. Wu, D. Okaya, B.-S. Huang, and W.-T. Liang (2009), SKS/SKKS splitting and Taiwan orogeny, *Geophys. Res. Lett.*, *36*, L12303, doi:10.1029/2009GL038148.

1. Introduction

[2] Taiwan is created as a result of the oblique convergence between the Philippine Sea Plate (PSP) and the Eurasian Plate (EUP). PSP subducts northward under EUP along the Ryukyu Trench in northern Taiwan; however, in contrast EUP subducts eastward under PSP in southern Taiwan and behaves similarly along the Manila Trench farther to the south (Figure 1a). The relative plate motion between EUP and PSP is measured at 82 mm/yr in the N54°W direction [*Yu et al.*, 1997]. In central Taiwan, where collision has created mountains, the overall structural trend is N15°E. Southern Taiwan, south of about 23°N, overlies the EUP subduction zone and is nearly NS in strike, but in northern Taiwan where the subduction PSP terminates the structural trend turns sharply toward EW, subparallel to the Ryukyu arc.

[3] Eight tectonic units are generally recognized (Figure 1b) [*Ho*, 1986]. From east to west: the Coastal Range (CoR) is the compressed Luzon Arc and its forearc; the Longitudinal Valley (LV) separates CoR from the pre-Tertiary metamorphic Eastern Central Range (ECR) - LV being the suture between EUP and PSP; the Backbone Range (BR) is composed of Miocene to Eocene age slates; the Hsueshan Range (HR) is built from mostly Eocene and Oligocene continental shelf sediments from the west; the Western Foothills (WF) corresponds to the accreted and deformed sediments of the foreland basin; and the Coastal Plain (CP) is the present foreland basin [*Ho*, 1986]. In addition the Ilan Plain (IP) in northern Taiwan is apparently the western extension of the Okinawa Trough, a back-arc basin.

[4] The kinematic property in the upper mantle and crust related to lattice-preferred orientation (LPO) anisotropy, as revealed by shear wave splitting, can be linked directly to deformation. The splitting parameters of the fast wave polarization direction (φ) and delay time (δt) provide the orientation and the product of magnitude and the path length, respectively, of LPO in the mantle [e.g., *Silver*, 1996]. The origin of anisotropy may differ according to tectonic regime [e.g., *Park and Levin*, 2002]. Generally, in non-collisional or non-plate boundary regions φ will be parallel to the direction of the absolute plate motion (i.e., mantle flow), and the source of anisotropy is mainly from the flow of the upper mantle. However, in active collisional orogens large δt (1.0–2.4s) are often observed, and φ generally aligns with the strike of the mountain belts such as Tibet and New Zealand [*Silver*, 1996; *Park and Levin*, 2002]. Because δt for crustal events are usually less than a few tenths of a second, and because the lower mantle is not likely to be the source of splitting, the observed δt of one to two seconds must be produced in the upper mantle [*Silver*, 1996]. The correlation between the surface structural trend and the possible mantle LPO anisotropy has been widely referred to as the vertically coherent deformation of the crust and upper mantle [*Silver*, 1996]. On the other hand, in subduction systems, φ varies with the tectonic conditions of a region (either parallel or normal to the strike of the trench). Several possible explanations have been proposed: the direction of mantle flow [*Russo and Silver*, 1994; *Su and Park*, 1994], dehydration-related LPO in olivine [e.g., *Bowman and Ando*, 1987; *Peyton et al.*, 2001; *Jung and Karato*, 2001], and trench parallel faulting in the subduction slab [*Faccenda et al.*, 2008]. Since Taiwan is situated in the vicinity of both a collision and a subduction zone the source of splitting can be expected to be more complex.

[5] Based on the splitting of S and ScS waves recorded at broadband and short period stations, *Rau et al.* [2000] determined the fast directions and delay times at many stations across the island. *Huang et al.* [2006] on the other hand used SKS waves from one African event recorded on a line of stations across southern Taiwan (Figure 2). Although both studies found φ to be sub-parallel to the structural trend, there is a discrepancy between δt from *Rau et al.* [2000] (>1.0sec) and *Huang et al.* [2006] (<0.6 sec) in the Coastal Plain. We shall look at more data in this area and

[1]Department of Geological Sciences, State University of New York at Binghamton, Binghamton, New York, USA.
[2]Department of Earth Sciences, University of Southern California, Los Angeles, California, USA.
[3]Institute of Earth Sciences, Academia Sinica, Taipei, Taiwan.

0094-8276/09/2009GL038148

see whether the discrepancy persists and what may be the cause(s) for it.

[6] The recent TAIGER (Taiwan Integrated Geodynamics Research) deployment of a temporary broadband seismic array densifies coverage provided by the existing permanent networks in Taiwan (Figure 1b). We also found that SKKS phase is well recorded from South American earthquakes. The splitting results at our new sites better clarify the spatial distribution of φ and δt in the different tectonic units and allow us to relate them to possible sources of anisotropy in the upper mantle.

2. Data and Analysis

[7] We use data from three separate broadband networks that were in operation during 1996–2008. In 1995 BATS (Broadband Array in Taiwan for Seismology) began to install STS-1 and STS-2 based systems in permanent vaults; the total number of stations is 17. In 2001 CWB (Central Weather Bureau) began their broadband network with Guralp sensors, for a total of 36. And finally the temporary TAIGER stations with Guralp sensors were installed in shallow subsurface holes The deployment began in April 2006 and reached 47 stations in October 2007, and they were taken out in May 2008. The TAIGER stations are distributed mainly along three transects with additional sites in the Central Range of northeastern Taiwan (Figure 1b).

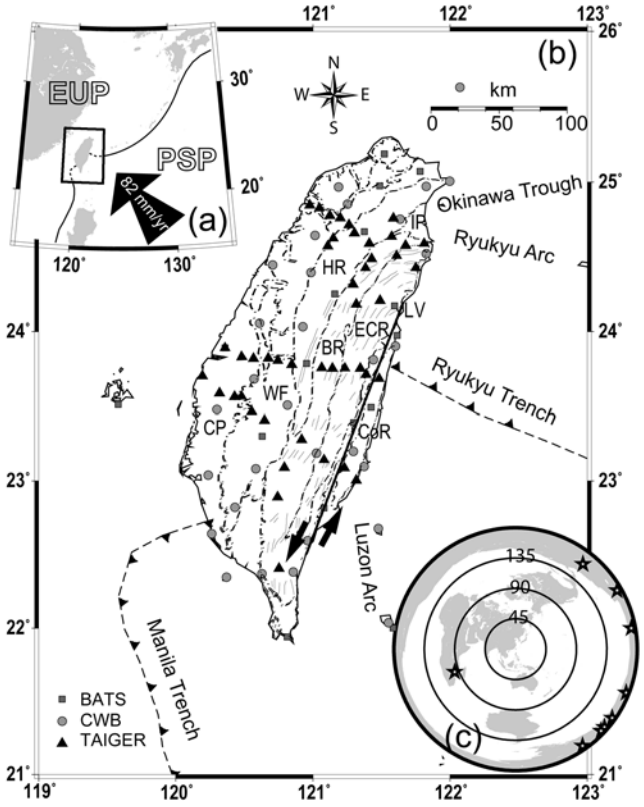

Figure 1. (a) Taiwan plate boundary. (b) Tectonic setting of Taiwan. Short clusters of sub-parallel line segments in ECR, BR, and HR regions represent strikes of foliations. (c) Stars indicate the azimuthal distribution of earthquakes used in this study. Taiwan is at center, radial distance is in degrees.

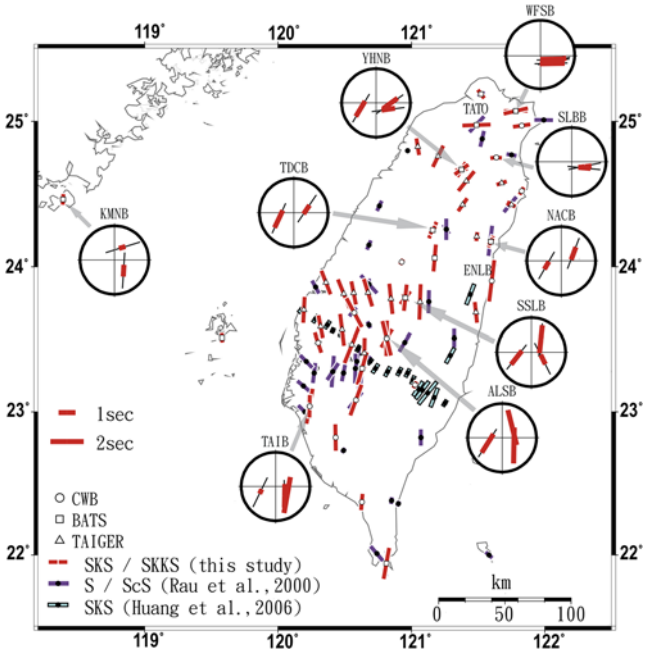

Figure 2. Combined splitting parameter results. φ follow local structural trends and are parallel to the orogen. The stereoplots show splitting parameters at a station for different event back-azimuths. The thin black bar indicates φ. The thick red bar represents δt. The distance from the center to the edge of the stereoplot shows the inclination of the teleseismic earthquake (vertical to 20°).

During 1996–2008 the island had a fairly dense coverage (Figure 1b).

[8] SKS/SKKS phases are commonly used for S-splitting measurements because their splitting is caused only by receiver-side material anisotropy [*Silver*, 1996]. Taiwan is not at an optimal location to receive SKS/SKKS from the active seismic zones of the world. However, from 2000 to 2008 we were able to identify well-isolated SKKS from 8 South American events and SKS from one African event (Figure 1c); a total of 58 new splitting measurements have been obtained (see Table S1 of splitting parameters in the auxiliary material).[1]

[9] We used the Rotation-Correlation method of *Bowman and Ando* [1987], performed with a 1° by half time-sampling rate grid-search for the parameters φ and δt. The Rotation-Correlation method uses the maximum of the cross-correlation coefficient between the waveforms on the radial and transverse components; the φ and δt at the maximum represent the values at which the particle motion becomes linear. Figure 3 shows examples of seismograms analyzed by using SplitLab, a Matlab program developed by *Wüstefeld et al.* [2008], in which the maxima of the cross-correlation coefficients are indicated. *Levin et al.* [2007] has tested the different methods used to measure splitting parameters and the Rotation-Correlation method is found to be suitable for cases where delay times are large. Seismo-

[1]Auxiliary materials are available in the HTML. doi:10.1029/2009GL038148.

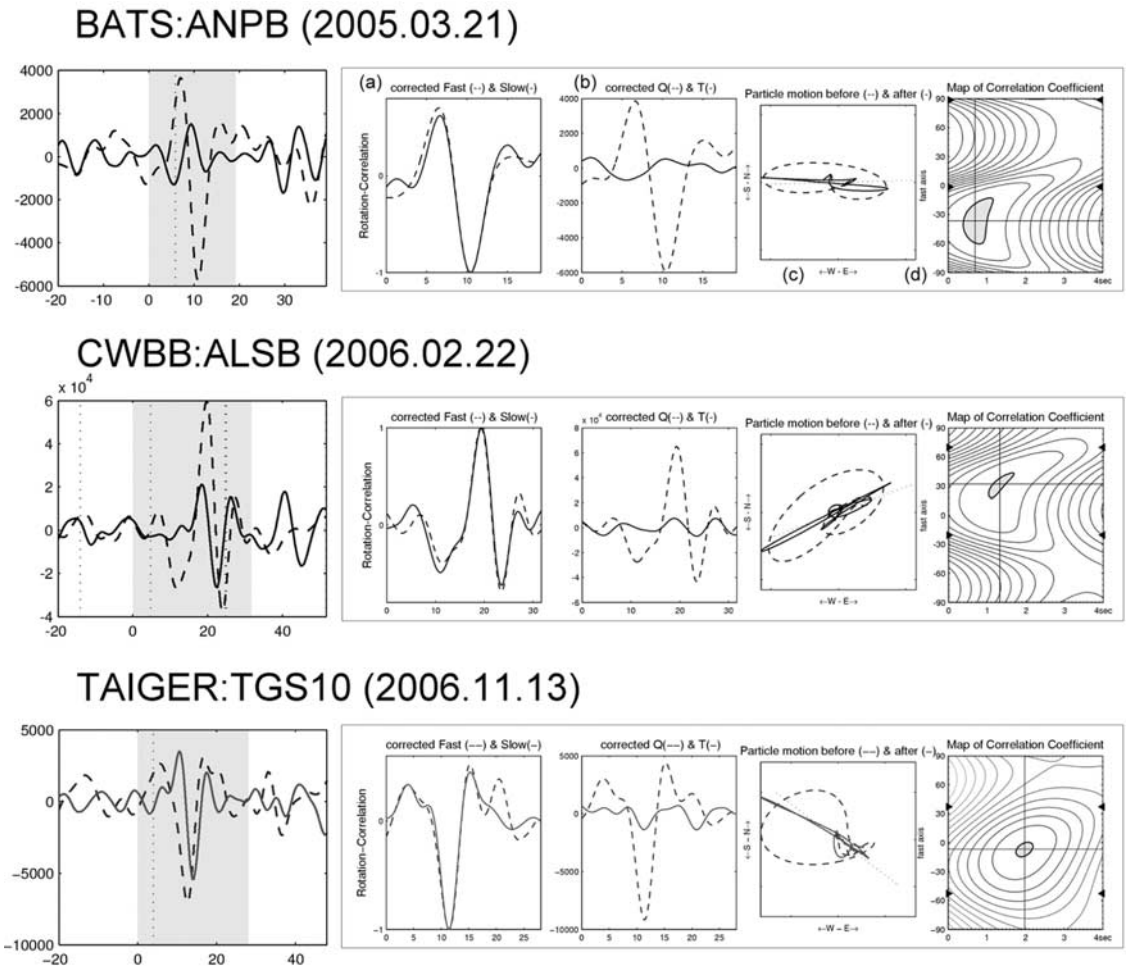

Figure 3. Examples of splitting measurements from different networks. For each event: SKS-windowed seismogram radial (Q, solid) and transverse (T, dashed) components before anisotropy Rotation-Correction; Seismogram components in fast (solid) and slow (dashed) directions; Q and T components after Rotation-Correction (not normalized); particle motion before (dashed) and after (solid) Rotation-Correction; and contour plot of correlation coefficients.

grams were band-pass-filtered at 0.02–0.2 Hz in order to remove unwanted noise.

3. Results

[10] Figure 2 shows the splitting parameters φ and δt of this study and of previous works from *Rau et al.* [2000] and *Huang et al.* [2006]. Although the new and the previous results largely agree in terms of overall fast directions, most of the delay times from our new results are noticeably greater than *Huang et al.* [2006] and the addition of new data more clearly defines the patterns of φ around major structures, especially in the southwest and north. The average δt in Taiwan is 1.3 seconds with its maximum (2.6 sec) at station ENLB near the northern end of the Coastal Range and its minimum (0.3 sec) at TAIB in southwestern Taiwan. In general, φ in central and southern Taiwan (roughly 22.5°N to 24°N) correlate well with local structural trends (Figure 2). There are two other salient features observed in this study. First, a comparison of δt from this study with those of *Huang et al.* [2006] in southern Taiwan shows δt from the directions of SE and SW incoming ray paths are 1.4–2.0 sec and 0.2–0.6 sec, respectively (Figure 2). Secondly, with the addition of TAIGER stations in northern Taiwan, the gradual change in φ from N–NNE in southern and central Taiwan to EW in northern Taiwan is clearly recognizable (Figure 2).

4. Discussion and Conclusion

[11] The concordance of φ with the structural trend and the magnitude of δt of S-splitting throughout the whole island resemble those of other continental mountain ranges such as western Tianshan [*Makeyeva et al.*, 1992], Tibet [*McNamara et al.*, 1994] and New Zealand [*Klosko et al.*, 1999]. These observations led *Silver* [1996], *Barruol et al.* [1998], *Molnar et al.* [1999] and others to propose vertical coherent tectonics to extend from the surface to a depth of several hundred kilometers. In the case of Taiwan, because rocks in the Backbone Range and East Central Range are highly foliated [*Lee*, 1997] and may have more than 25% anisotropy based on laboratory velocity measurements where φ aligns with the metamorphic foliation (Figure 1b) [*Christensen et al.*, 2006], the additional delay due to crustal anisotropy may need to be considered. However, the measured crustal splitting in Taiwan yields a maximum delay of

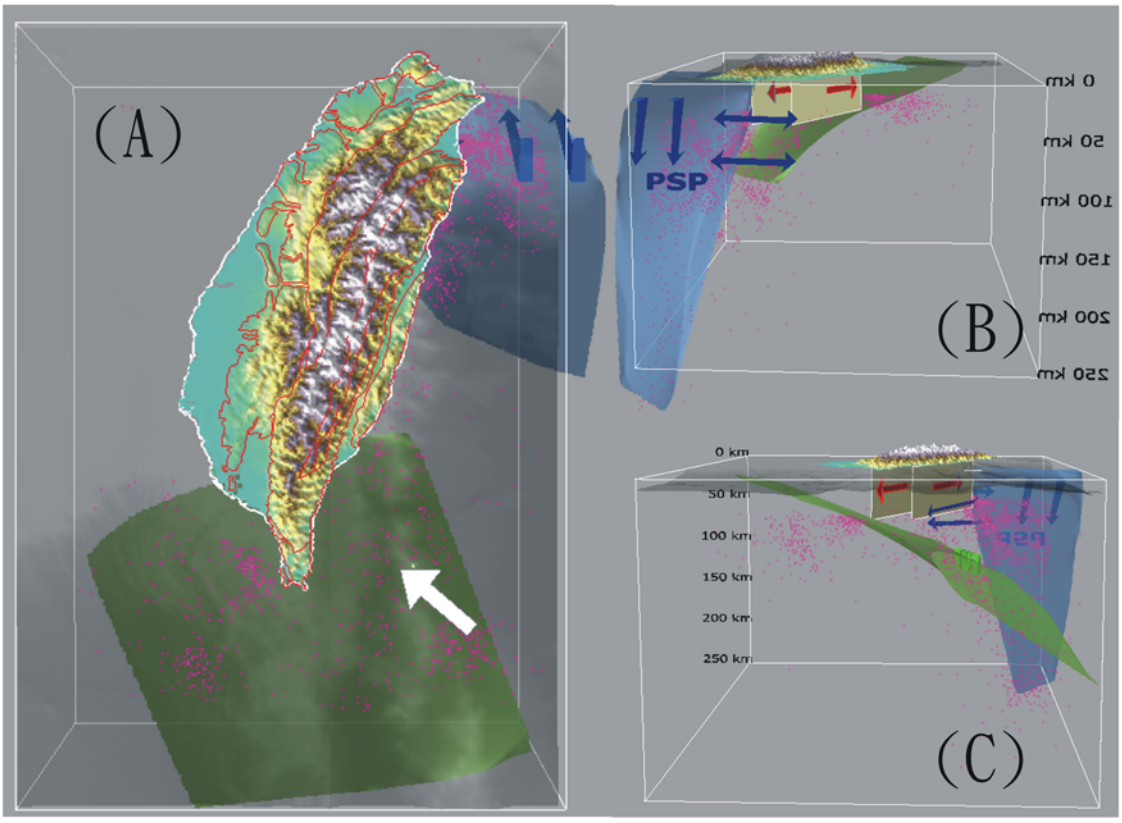

Figure 4. Schematic figure demonstrating the possible sources of anisotropy in Taiwan shown in (a) map view, (b) side view from north looking south, and (c) side view from south looking north. In central and southern Taiwan, the source of the anisotropy is mainly from the vertically coherent deformation of the crust and upper mantle by left-lateral shearing. Red arrows represent the shear directions. In northern Taiwan, the source of anisotropy may be more complicated. Both hydrated olive in the upper mantle and the extrusion at the end of a collision zone are possible sources, but other possibilities can not be excluded. Blue arrows represent the possible directions of mantle flow and extrusion. Blue and green surfaces are PSP and EUP slab tops, respectively. Red lines are geological boundaries. Pink dots are earthquakes larger than magnitude 3.5 and depth deeper than 40 km from the CWB earthquake catalogue (1990∼2007). The white arrow is the relative plate motion. The vertical scale of topography and bathymetry is enlarged by 5. See Animation S1 in the auxiliary material for an animation of the schematic.

less than 0.4 second [*Kuo et al.*, 1994; R.-J. Rau, personal communication, 2004; H. Kuo-Chen et al., S-Splitting Measurements and Taiwan Orogeny, paper presented at the 2008 IRIS workshop, Incorporated Research Institutions for Seismology, Stevenson, Washington, 4–6 June 2008] and also *Marson-Pidgeon and Savage* [1997] have considered that the factor of frequency dependent anisotropy; the frequencies of crustal earthquakes would contribute δt around 0.5 sec. Hence, the 1–2.6 second delays that we obtained imply that the major source of anisotropy resides in the upper mantle.

[12] In terms of the mechanisms discussed in the introduction that create LPO anisotropy, two tectonic processes in the crust and upper mantle under Taiwan can contribute to the observed splitting. In central and southern Taiwan, because of the obliquity of the PHP-EUP collision the trend-perpendicular shortening is accompanied by left-lateral shear, which is evidenced at the surface by left-lateral strike-slip motion along the Longitudinal Valley [*Chang et al.*, 2000] (Figure 1b). Since φ in these areas are parallel or sub-parallel to the shear direction a vertically coherent shear zone may have produced the LPO (Figure 4). Assuming an intrinsic shear wave velocity anisotropy of 4%, one second of δt corresponds to an anisotropic layer thickness of 115 km. This suggests an anisotropic layer thickness of about 250 km in the upper mantle under central and southern Taiwan.

[13] In contrast to central and south-central Taiwan, both the southernmost (21.7 to 22.5°N) and the northernmost (24°N to 25.5°N) regions of the island overlie subduction zones (Figures 1b and 4) [*Wu et al.*, 1997]. It is commonly recognized that convergence-parallel φ may be associated with different geophysical or geochemical properties in subduction zones and have been recently summarized by *Behn et al.* [2007] and *Faccenda et al.* [2008]. In southernmost Taiwan we obtained a δt of approximately one second with φ parallel to the trend of Taiwan (the Luzon Arc and Manila Trench). Our southernmost Taiwan measurement is located over the relatively flat portion of the subducting EUP slab under what is nominally PSP (Figure 4). With the absolute plate motion (in the HS3-NUVEL 1A framework) of EUP in the direction of S65°E, the global mantle flow patterns are not a likely cause. φ that are arc-trench parallel to southernmost Taiwan may indicate

that the NW direction of PSP mantle flow is impeded by the central and southern Taiwan collision zone (lithospheric root) and diverts the mantle flow to the NS direction.

[14] On the other hand, in northern Taiwan (24°N to 25.5°N) the structural trend at the surface turns nearly EW, a phenomenon often explained as a result of the termination of the Ryukyu subduction/collision zone in northern Taiwan [e.g., *Wu et al.*, 1997]. This EW rotation is akin to that of the eastern syntaxis of the Himalayas as a region of extrusion at the end of a collision zone [*Sol et al.*, 2007]. In northern Taiwan the measured φ turn from orogen-parallel to nearly Ryukyu-arc-parallel, and the associated δt's show a general increase toward the north (Figure 2). The maximum δt of 1.8 sec is found at TATO (Figure 2). This remarkable rotation of φ correlates with the structural patterns at the surface (Figure 2). The EW fast direction has also been observed in the Ryukyu Islands as reported by *Long and van der Hilst* [2006]; they hypothesized that hydrated olivine and convection flow under the back-arc basin [e.g., *Honda et al.*, 2002] was responsible for this orientation. In northern Taiwan the situation is more complex; here the Ryukyu subduction system terminates, with the subducted PSP continuing on its northwestward motion relative to EUR, and PSP with EUR are no longer in collision as PSP submerges under EUR. A flow around PSP as it advances against EUR in the upper mantle or an "escape flow" at the end of the collision zone (Figure 4) may all contribute to the EW-orientation of φ in this region.

[15] From the inspection of δt observed across Taiwan in previous studies [*Rau et al.*, 2000; *Huang et al.*, 2006] and in our own data, we can detect significant variations, especially in southern Taiwan with data from different back-azimuths. The inset stereonets for TAIB, ALSB and SSLB (Figure 2) show the split results as a function of back-azimuth, inclination (or distance) and station average δt. Although the back-azimuth dependence of splitting parameters may indicate complicated fabric underneath the Taiwan orogen, the measurements from this study do not have sufficient azimuthal coverage to do the full analysis proposed by [*Savage*, 1999]. However, by approximating this region as a single laterally varying anisotropic layer and taking into consideration the Fresnel zone of the incoming waves, the EW asymmetry in split time indicates that below about 60 km the incoming SKS/SKKS waves can discriminate the highly anisotropic region under the Backbone Range and East Central Range from the less anisotropic zone of southwestern Taiwan.

[16] **Acknowledgments.** We thank the staff of the Seismology Center of the Central Weather Bureau and the Institute of Earth Sciences, Academia Sinica, for providing earthquake data. This study is supported by a grant from the NSF Continental Dynamics program (EAR-0410227). Also, this work is supported by a Ph.D. scholarship from the Ministry of Education of Taiwan to H.K-C.

References

Barruol, G., A. Souriau, A. Vauchez, J. Diaz, J. Gallart, J. Tubia, and J. Cuevas (1998), Lithospheric anisotropy beneath the Pyrenees from shear wave splitting, *J. Geophys. Res.*, *103*, 30,039–30,053.

Behn, M. D., G. Hirth, and P. B. Kelemen (2007), Lower crustal foundering as a mechanism for trench parallel seismic anisotropy below volcanic arcs, *Science*, *317*, 108–111.

Bowman, J. R., and M. Ando (1987), Shear-wave splitting in the upper-mantle wedge above the Tonga subduction zone, *Geophys. J. R. Astron. Soc.*, *88*, 25–41.

Chang, C.-P., J. Angelier, and C.-Y. Huang (2000), Origin and evolution of a melange: The active plate boundary and suture zone of the Longitudinal Valley, Taiwan, *Tectonophysics*, *325*, 43–62.

Christensen, N., D. Okaya, and A. Meltzer (2006), The nature of crustal seismic anisotropy: Constraints from field and rock physics observations, *Eos Trans. AGU*, *87*(52), Fall Meet. Suppl., Abstract T52B-03.

Faccenda, M., L. Burlini, T. V. Gerya1, and D. Mainprice (2008), Fault-induced seismic anisotropy by hydration in subducting oceanic plates, *Nature*, *455*, 1097–1100.

Ho, C. S. (1986), *An Introduction to the Geology of Taiwan: Explanatory Text of the Geologic Map of Taiwan*, Cent. Geol. Surv., Taipei.

Honda, S., M. Saito, and T. Nakakuki (2002), Possible existence of small-scale convection under the back arc, *Geophys. Res. Lett.*, *29*(21), 2043, doi:10.1029/2002GL015853.

Huang, B.-S., W.-G. Huang, W.-T. Liang, R.-J. Rau, and N. Hirata (2006), Anisotropy beneath an active collision orogen of Taiwan: Results from across islands array observations, *Geophys. Res. Lett.*, *33*, L24302, doi:10.1029/2006GL027844.

Jung, H., and S.-I. Karato (2001), Water-induced fabric transitions in olivine, *Science*, *293*, 1460–1463.

Klosko, E. R., F. T. Wu, H. J. Anderson, D. Eberhart-Phillips, T. V. McEvilly, E. Audoine, M. K. Savage, and K. R. Gledhill (1999), Upper mantle anisotropy in the New Zealand region, *Geophys. Res. Lett.*, *26*, 1497–1500.

Kuo, B., C. Chen, and T. Shin (1994), Split S waveforms observed in northern Taiwan: Implications for crustal anisotropy, *Geophys. Res. Lett.*, *21*, 1491–1494.

Lee, Y. H. (1997), Structural evolution of the middle Central Range during the Penglai orogeny, Taiwan, Ph.D. thesis, Natl. Taiwan Univ., Taipei.

Levin, V. D., D. Okaya, and J. Park (2007), Shear wave birefringence in wedge-shaped anisotropic regions, *Geophys. J. Int.*, *168*, 275–286.

Long, M. D., and R. D. van der Hilst (2006), Shear wave splitting from local events beneath the Ryukyu arc: Trench-parallel anisotropy in the mantle wedge, *Phys. Earth Planet. Inter.*, *155*, 300–312.

Makeyeva, L. K., L. P. Vinnik, and S. W. Roecker (1992), Shear-wave splitting and small scale convection in the continental upper mantle, *Nature*, *358*, 144–147.

Marson-Pidgeon, K., and M. K. Savage (1997), Frequency-dependent anisotropy in Wellington, New Zealand, *Geophys. Res. Lett.*, *24*, 3297–3300.

McNamara, D. E., T. J. Owens, P. G. Silver, and F. T. Wu (1994), Shear wave anisotropy beneath the Tibetan Plateau, *J. Geophys. Res.*, *99*, 13,655–13,665.

Molnar, P., et al. (1999), Continuous deformation versus faulting through the continental lithosphere of New Zealand, *Science*, *286*, 516–519.

Park, J., and V. Levin (2002), Seismic anisotropy: Tracing plate dynamics in the mantle, *Science*, *296*, 485–489.

Peyton, V., V. Levin, J. Park, M. Bradon, J. Lees, E. Gordeev, and A. Ozerov (2001), Mantle flow at a slab edge: Seismic anisotropy in the Kamchatka region, *Geophys. Res. Lett.*, *28*, 379–382.

Rau, R.-J., W.-T. Liang, H. Kao, and B.-S. Huang (2000), Shear wave anisotropy beneath the Taiwan orogen, *Earth Planet. Sci. Lett.*, *177*, 177–192.

Russo, R. M., and P. G. Silver (1994), Trench-parallel flow beneath the Nazca plate from seismic anisotropy, *Science*, *263*, 1105–1111.

Savage, M. K. (1999), Seismic anisotropy and mantle deformation: What have we learned from shear wave splitting?, *Rev. Geophys.*, *37*, 65–106.

Silver, P. G. (1996), Seismic anisotropy beneath the continents: Probing the depths of geology, *Annu. Rev. Earth Planet. Sci.*, *24*, 385–432.

Sol, S., et al. (2007), Geodynamics of the southeastern Tibetan Plateau from seismic anisotropy and geodesy, *Geology*, *35*, 563–566.

Su, L., and J. Park (1994), Anisotropy and the splitting of PS waves, *Phys. Earth Planet. Inter.*, *86*, 263–276.

Wu, F. T., R. J. Rau, and D. H. Salzberg (1997), Taiwan orogeny: Thin skinned or lithospheric collision?, *Tectonophysics*, *274*, 191–220.

Wüstefeld, A., G. H. R. Bokelmann, C. Zaroli, and G. Barruol (2008), SplitLab—A shear wave splitting environment in Matlab, *Comput. Geosci.*, *34*, 515–528.

Yu, S.-B., H.-Y. Chen, and L.-C. Kuo (1997), Velocity field of GPS stations in the Taiwan area, *Tectonophysics*, *274*, 4–59.

B.-S. Huang and W.-T. Liang, Institute of Earth Sciences, Academia Sinica, P.O. Box 1-55, Nankang, Taipei 115, Taiwan.

H. Kuo-Chen and F. T. Wu, Department of Geological Sciences, State University of New York at Binghamton, P.O. Box 6000, Binghamton, NY 13902-6000, USA. (kuochen.hao@gmail.com)

D. Okaya, Department of Earth Sciences, University of Southern California, 133 Couth Science Building, Los Angeles, CA 90089-0740, USA.